

# HARDWARE IN-THE-LOOP SIMULATIONS OF A NAVIGATION CAMERA IN A COMETARY DUST ENVIRONMENT

Christina Toldbo<sup>(1)</sup>, Jesper Henneke<sup>(1)</sup>, Robin Courson<sup>(2)</sup>, John Leif Jørgensen<sup>(1)</sup>, Per Bodin<sup>(2)</sup>

<sup>(1)</sup>*DTU Space, Danish Technical University, Kgs. Lyngby, 2800, Copenhagen Region, Denmark*

<sup>(2)</sup>*AOCS Department at OHB Sweden AB, Kista, Stockholm, Sweden*

## ABSTRACT

This paper presents a novel Hardware-In-the Loop (HIL) simulation tool with the capability to accurately and realistically test the response of optical systems during a fly-by of a comet through the central coma region i.e. in a heavy dust environment. The HIL simulations are performed using the Dynamic Optical Ground Support Equipment (DOGSE) developed at DTU Space which can expose representative optical sensors to high fidelity, dynamic, optical stimulations on a small, high-resolution screen. The DOGSE tool enable flexible, yet complex HIL simulation tests of mission scenarios with a fast turn-around and realistically display the translucent coma against an accurate projection of the starry sky. The tool takes as its input a trajectory file and generate synthetic images of the comet based on a cometary dust distribution model in the vicinity of the comet nucleus. This paper presents current developments and results based on the navigation architecture of the Comet-I mission.

## 1 INTRODUCTION

Comet nuclei are small, dark (albedo  $< 0.07$ ) and often irregular bodies composed of dust, rock, and ice. When a comet approaches the Sun, it heats up and ice begins to sublimate of the nucleus forming three distinct comet features:

1. The roundish coma (comet head) thousands of times larger than the nucleus (varying in size as a function of the distance to the Sun)
2. An anti-sunward, curved, fan-shaped dust tail, millions of kilometres long, resulting from the solar radiation pressure and the gravitational pull of the nucleus and the Sun acting on the emitted dust particles
3. A plasma tail arising from the ionization of gas molecules.

Comets are of high scientific interest as they are made of pristine material dating back to the formation of the solar system. For this reason, a number of missions have flown by comets at various distances and collected valuable data and images (e.g. Giotto [1], Deep Space [4], Deep impact [6]) and samples of the dust (Stardust [8]). In 2014 the Rosetta spacecraft became the first mission to orbit a comet and its probe Philae became the first to land on a comet [12].

The brightness and appearance of a comet depends on the dust environment which in turn is related to the size of the nucleus, the out-gassing rate, the viewing geometry and whether the comet is dynamically new or not (a dynamically new comet has not previously passed the Sun). The Comet-I mission,

set for launch in 2029, aims to intercept a presently unknown comet or potentially an interstellar body and will fly within a distance of 1000 km from the nucleus.

Comet-I is a highly complex and dynamic mission which, at closest approach, rely on the optical navigation and autonomous on-board guidance to point towards the comet nucleus and optimise data acquisition and scientific output. Accurate and robust navigation sensors are key for mission success and flexible and representative methods for testing them are of high value.

Because the target is unknown extensive testing against a broad range of possible mission scenarios, target bodies and dust environments is needed. In addition, the target comet may still not be known at launch and testing will likely be necessary during flight when a specific target is being considered or pursued, requiring the testbed to be highly flexible and cost-efficient. The nature of comets and the distances/scales involved make it infeasible to construct a physical test-setup and a purely simulated environment would lack the hardware in the loop. Fortunately, for optical systems, a hybrid solution exists where the cameras are stimulated with simulated scenes on a screen, thus retaining the hardware in the loop and increasing the representativeness of the test bench, while still being cost-effective and flexible.

## 2 THE COMET-I MISSION AND THE CHALLENGES IT PRESENTS TO OPTICAL NAVIGATION

The general concept for the Comet-I mission is to park the spacecraft in the Sun-Earth L2 Lagrange point where it will await an interesting candidate for interception [14]. The spacecraft will then catch up with the comet/interstellar body and pass the comet nucleus at close proximity ( $\sim 1000$  km) at high relative velocity (15–70 km/s). Figure 1 shows a sketch the encounter geometry.

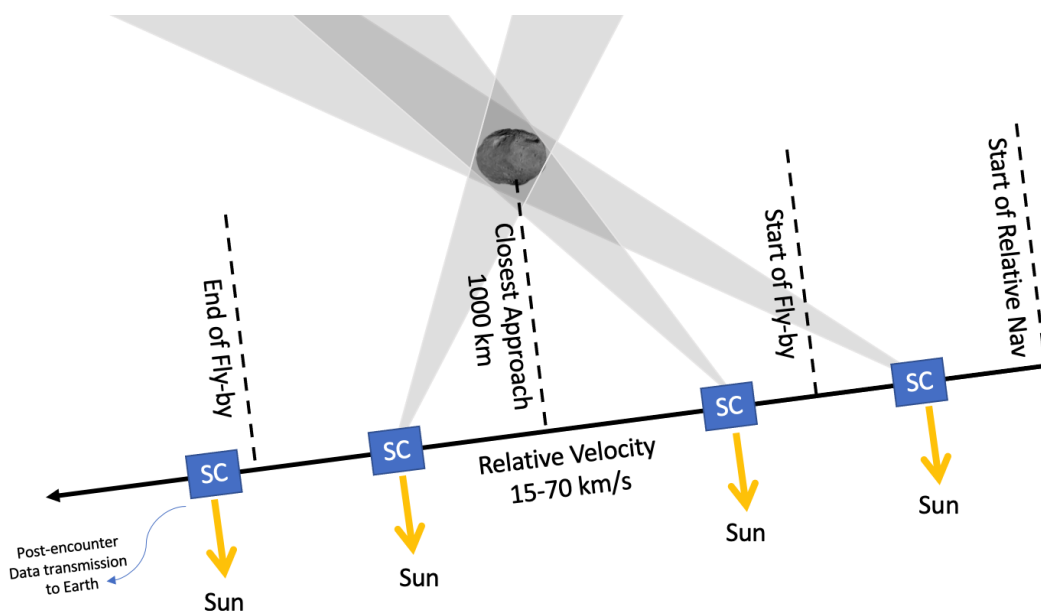


Figure 1: Sketch of the trajectory of the Comet-I spacecraft (SC) during the interception of the comet. The spacecraft will pass between the Sun and the comet and will fly through the inner dust region at a distance of approximately 1000 km from the nucleus. Adapted from [15].

Common for previous missions is that they have had specific comet(s) as their intended target prior to launch. The target comets have been observed several years in advance when passing the Sun and their dust environment and trajectories have been approximately known. The Comet-I mission will on the other hand be challenged by to the inherent uncertainties associated with intercepting the a priori unknown, fast-moving comet.

The spacecraft must be designed to operate successfully both if little or no dust is present, as well as in a potential dense cloud of gas and dust. The primary challenges to the optical navigation system in a dusty environment are:

- The challenges presented by the comet being a priori unknown and limited flight experience in the vicinity of comets
- The need for a bumper shield and mitigation strategy when the spacecraft is impacted by dust grains.

Only seven comets (1P/Halley, 19P/Borrelly, 9P/Tempel 1, 26P/Grigg-Skjellerup, 67P/Churyumov-Gerasimeko, 81P/Wild 2, and 103P/Hartley 2) have been visited by spacecraft [17]. Images from these missions (available from [5], [7]) have unveiled that comets are complex objects with an often irregularly shaped nuclei and periodic, directional jets and streams of dust and gas. Figure 2 shows images taken by the Rosetta mission to comet 67P/Churyumov-Gerasimeko at different distances and showcase the irregularity of the nucleus and the directional jets (in the last two images).

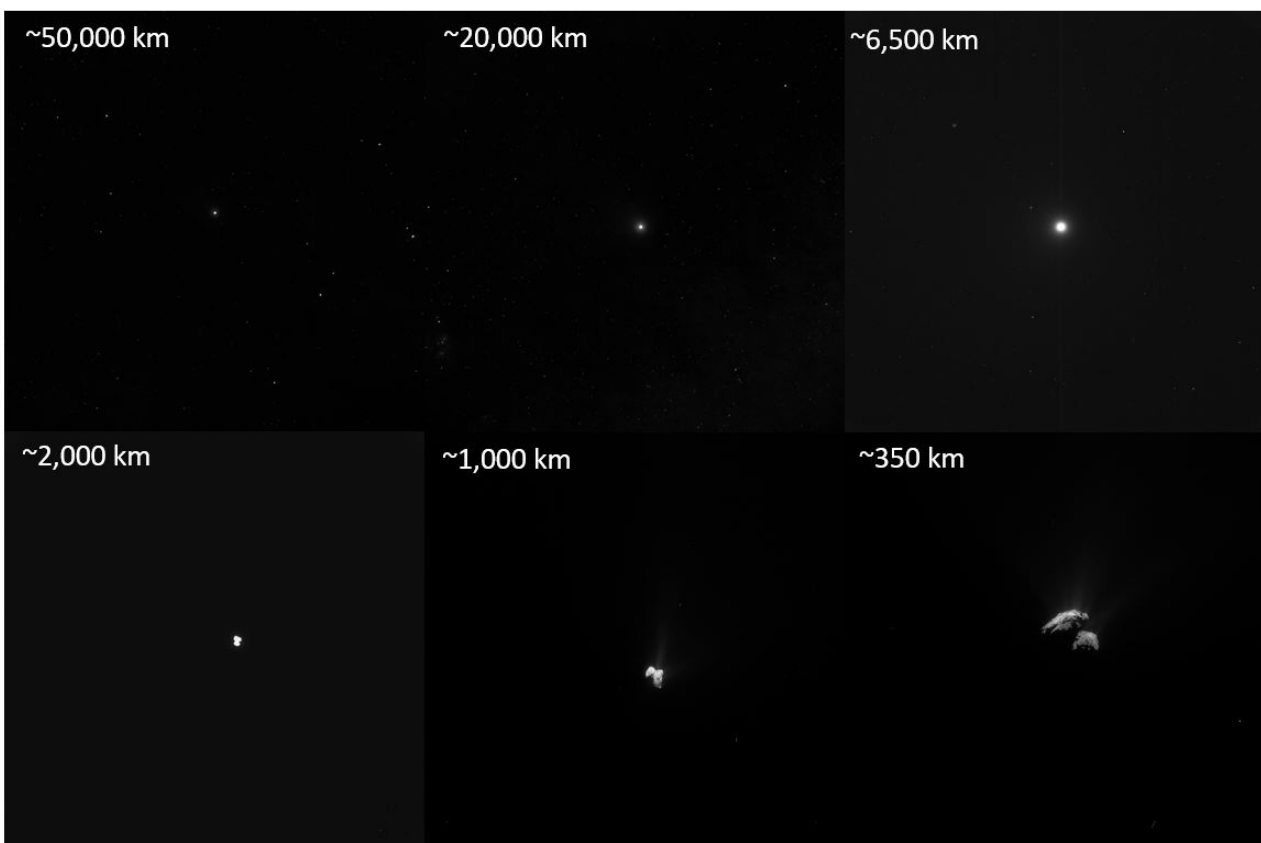


Figure 2: Rosetta Images of Comet 67P/Churyumov-Gerasimenko taken by Navigation Camera 1 at different distances. The nucleus of 67P/Churyumov-Gerasimenko is approximately 3x5 km and the FOV of NAVCAM 1 is 5x5 degrees (focal length 152.5 mm) [7]. Image Credit: ESA/Rosetta/NAVCAM – CC BY-SA IGO 3.0

Figure 3 shows a similar sequence from the Giotto mission which passed within 596 km of Comet Halley in 1990. Comet Halley has a much bigger nucleus than 67P/Churyumov-Gerasimenko and a higher out-gassing rate [11] and displays a fan-shaped dust profile at large distances.

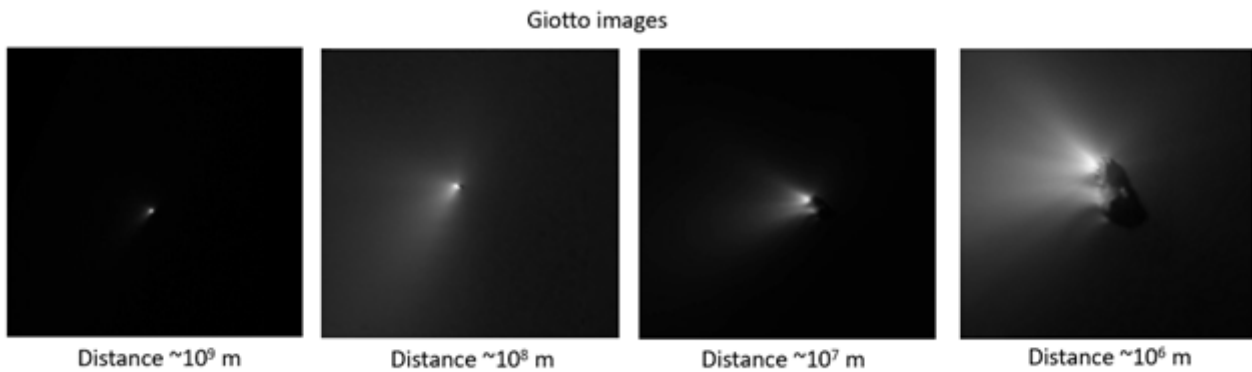


Figure 3: Images of Halley’s Comet at different distances taken by the Halley Multicolour Camera (HMC) on board ESA’s spacecraft Giotto. ©MPAe/MPS 1986, reprinted with permission from Max-Planck-Institut für Sonnensystemforschung, Göttingen, Germany. Raw images can be found from [5]

Data from the Giotto mission showed that the spacecraft was very sensitive to discrete attitude variations caused by particles in the 1-50 mg range [2] and the Multi-color Camera (HMC) on Giotto was lost by a direct hit by a particle.

To handle the above described challenges, Comet-I will be equipped with a number of narrow and wide angle navigation cameras in addition to star trackers for attitude determination. Essential cameras for close proximity navigation will be positioned behind ‘bumper shields’. Extensive test of the ability of the navigation systems to reacquire a lock after attitude disturbances is crucial.

### 3 THE DYNAMICAL GROUND OPTICAL SUPPORT EQUIPMENT

The Dynamic Optical Ground Support Equipment (DOGSE) for high fidelity virtual scene generation has been developed over the last years at DTU Space to enable flexible, yet complex test of vision-based sensors. The DOGSE consist of a small OLED (Organic Light Emitting Diode) micro-display positioned inside a lens barrel (see Figure 4) and an external computer running the DTU-developed software ‘Spazio’ which provide a GUI for the user to control the scene generation, settings, calibration and automation.

During test, the camera is inserted into the DOGSE barrel and connected with the Digital Processing Unit (DPU). The input to the DOGSE is one or more 3D models/synthetic images and a trajectory sequence containing the camera and target positions and attitudes. The output of the DOGSE system can be customized but as a baseline consist of the centroids and intensities of the locked stars and Non-Stellar Objects (NSOs) in the scene, the determined attitude as well as the raw images taken by the camera under test.

The DOGSE can be used ‘as is’ for a variety of test cases, spanning a wide range of mission objectives and scenarios. It can accurately project a user selected star catalogue as well as celestial objects and 3D models of e.g. spacecraft. The latter capability can be used to test and validate navigation sensors

for formation flight, rendezvous and docking with non-cooperative targets, relevant for example for clean space initiatives.

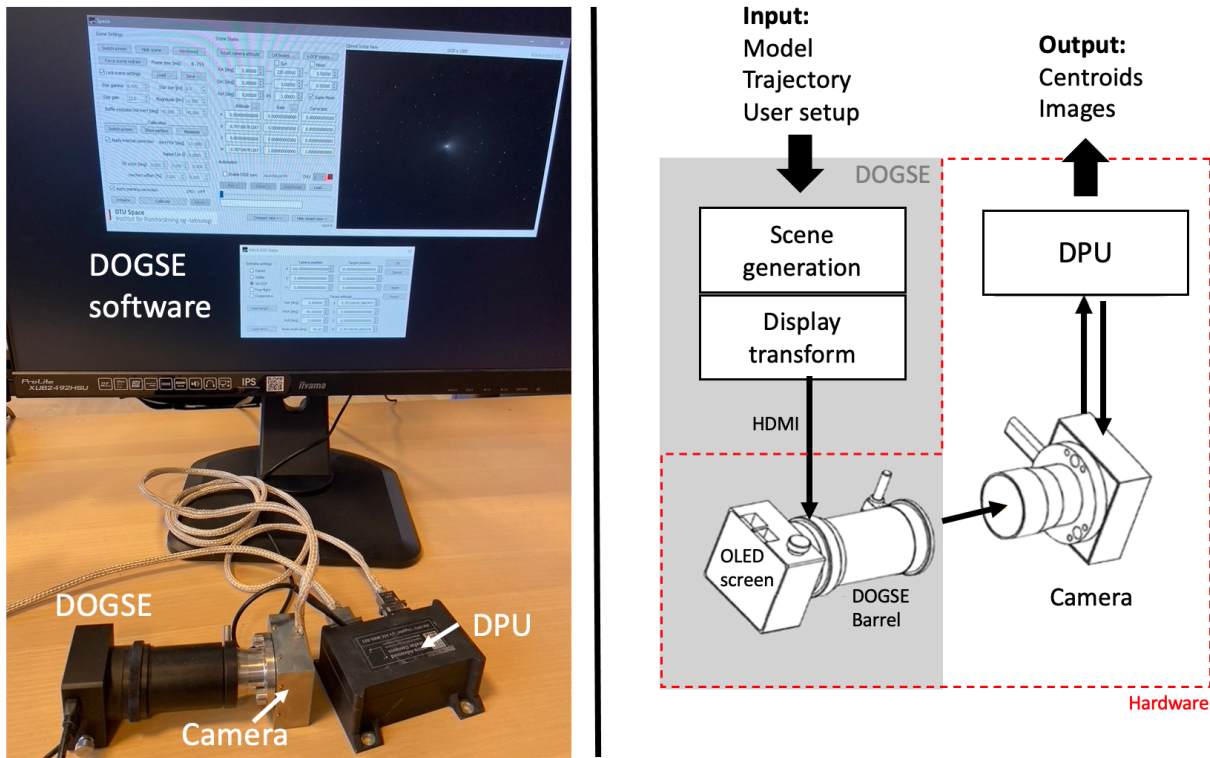


Figure 4: Left: The physical DOGSE test setup. Right: Sketch of the test setup and connections. The Camera is inserted into the DOGSE barrel which displays a simulated scene on the OLED screen inside. The scene rendering is controlled by a dedicated computer which facilitates the input and output generated during a simulation.

The DOGSE can be connected to any PC from which it is also possible to transmit images to the DOGSE screen directly via HDMI without the DOGSE GUI and software. As will be elaborated in the following section this allows customization for specific use cases where computational power, GPU and graphics card specs are of high importance – such as for near real time rendering.

#### 4 COMET RENDERING

Images returned from previous missions do not provide a substantially large basis for dynamic testing of different scenarios and thus synthetic images must be generated for the DOGSE. Rendering realistic images of a comet is however challenging for multiple reasons: unlike solid celestial objects, the semi-transparent, reflective coma presents difficulties as each gas and dust particle scatters and reflects sunlight, creating unique lighting conditions. It is not trivial to accurately represent the densities of particles inside the coma and simulating the interactions of light with the coma's transparent structure requires sophisticated rendering techniques to capture the delicate balance between transparency, reflectivity and light scattering. The dust distribution in the inner coma is mostly influenced by the initial velocities of the particles, but at larger distances the radiation pressure from the Sun plays a significant role. Accurately representing the outer coma and tails is challenging, and requires a thorough understanding of the dust dynamics.

Rendering the coma, which can stretch from very close to the observer to the nucleus in the far distance, requires careful consideration. The appearance of the comet changes significantly with distance, both in terms of shape and brightness. At large distance, the nucleus and its inner coma takes up less than a pixel in size and is best represented by a flux-equivalent disc, similar to how the stars are rendered in the scene: as a disc of which the integrated flux matches the luminous flux of a respective star.

## 4.1 Rendering engine options

Path tracing and rasterizer rendering are commonly used methods for rendering scenes. Path tracing provide accurate lighting and reflections using inverse tracing of the light rays from the camera, but is computationally expensive, making it less suitable for real-time rendering. Rasterizer rendering, on the other hand, prioritizes speed and efficiency, making it more appropriate for interactive or real-time scenarios like the ones suggested in this paper. This compromise means that we cannot use a real volumetric object and instead use a combination of solid, transparent-emissive objects to approach the appearance of the coma (see section 4.3).

## 4.2 Coma particle distribution and shading

### 4.2.1 Engineering Dust Coma Model

The Engineering Dust Coma Model (EDCM) (described in [17] and available from [16]) is based on a median case cometary activity after a study on several long-period comets. The model was developed to assess the impact of the pointing disturbances due to collisions with cometary particles at high relative velocities. The EDCM provides the densities of several grain sizes based on dust radii ('dust bins') but only along the spacecraft path.

Using reasonable symmetry assumption of the inner coma, it is possible to derive a global, low parameter model for each particle size bin. For a particle  $i$ , the derived density  $\rho$  at position  $\vec{p}$  depends on three constant parameters  $C_i$ ,  $K1_i$  and  $K2_i$ , as described below:

$$\rho(\vec{p}) = \frac{C_i}{\|\vec{p}\|^2} (1 + K1_i \cos \theta + K2_i \cos^2 \theta) \quad (1)$$

Where  $C_i$  describes the central density coefficient of the coma and  $K1_i$  and  $K2_i$  are additional coefficients that distort the coma shape as a function of the solar phase angle  $\theta$ .

### 4.2.2 Dust Particle Radiance

Each dust particle of radius  $r_i$  radiates the solar irradiance  $I_s$  received from the direction  $\vec{s}$  in the direction of the observer  $\vec{\omega}$  according to:

$$l_r(\vec{\omega}) = I_s \alpha(r_i) f(\vec{\omega}, \vec{s}, r_i) \quad (2)$$

Where  $\alpha(r_i)$  is the particle albedo (between 0 and 1) and  $f(\vec{\omega}, \vec{s}, r_i)$  is the normalized phase function, which depends only on the phase angle between the Sun, the particle and the observer. Analysis of several comets [10], [3] show that this phase function is usually far from an isotropic scattering.

### 4.2.3 Single bin model

Since we are only interested in the final radiance to the camera for our image generation purpose, we implement a single-bin, simplified model. If we consider only the central term  $C_i$  and we assume the same phase function across all dust bin, we can compute an equivalent  $C_{eq}, r_{eq}$  tuple such that:

$$C_{eq} r_{eq}^2 \alpha(r_{eq}) = \sum_i C_i r_i^2 \alpha(r_i) \quad (3)$$

Adding back the  $K1_i$  and  $K2_i$  coefficients, we can decide to introduce  $K1_{eq}$  and  $K2_{eq}$  as their respective medians over each dust bin  $i$ . This simplification is acceptable since  $K1_i, K2_i$  do not vary more than a factor 2 across the dust bins.

## 4.3 Implementation in a rendering software

Two different methods have been successively developed to render comet images at different relative positions.

### 4.3.1 CPU-based MATLAB custom renderer

The first implemented method relies on a custom MATLAB-written code implementing a simple rasterizer engine. This method uses the full dust bin range and integrates along the discretized line of sight of each pixel, adding the radiance contribution of each volumetric element. The sampling points are automatically chosen to minimize the error – hence, the sampling is denser where the coma density gradient is higher. The nucleus is modelled as a sphere in this approach and is rendered in a separate pass.

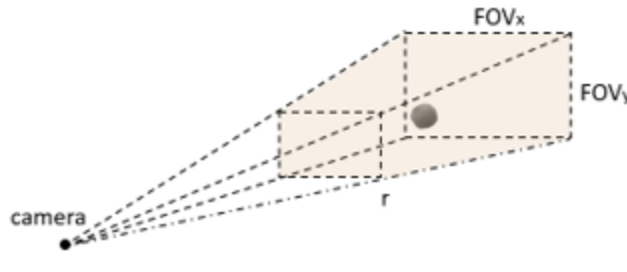


Figure 5: Sketch showing the integration along the line of sight of each pixel inside the field of view of the camera.

The main disadvantage of this method is that it is slow (CPU-based). The approach also does not offer much flexibility (i.e. any model addition, such as jets or a more complex nucleus model, is difficult).

### 4.3.2 GPU-based Blender renderer

To enable near real time, GPU-based rendering we use UPBGE (Uchronia Project Blender Game engine). UPBGE is a free open-source game engine based on the 3D content creation software Blender [13] which is often used for scientific visualization [9]. However, we have found no precedent for real-time scientific rendering based on UPBGE. This may be because volumetric rendering is not

properly supported in Blenders rasterizer engine (called EEVEE), thus presenting some challenges. However, volumetric rendering can be approximated by positioning a number of transparent, emissive planes around the comet nucleus, as seen in Figure 6.

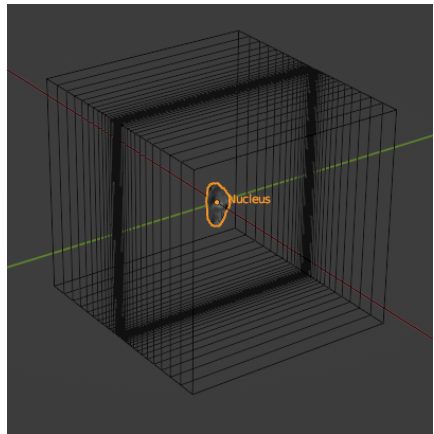


Figure 6: Planes positioned around the comet nucleus. The coma planes are typically positioned on a  $\pm 10^4 km$  axis and are about  $10^4 km$  in size, while the nucleus is only a few kilometers. In this figure the planes have been scaled down for the purpose of visualization.

A comparison of the coma radiance of this method versus the MATLAB multi-bins method is shown in Figure 7. The deviation in terms of relative radiance is in the order of 10% close to the nucleus where the coma is brightest. This is less than the uncertainties associated with working with an unknown comet and thus we argue that using the single bin model is a valid approach for testing.

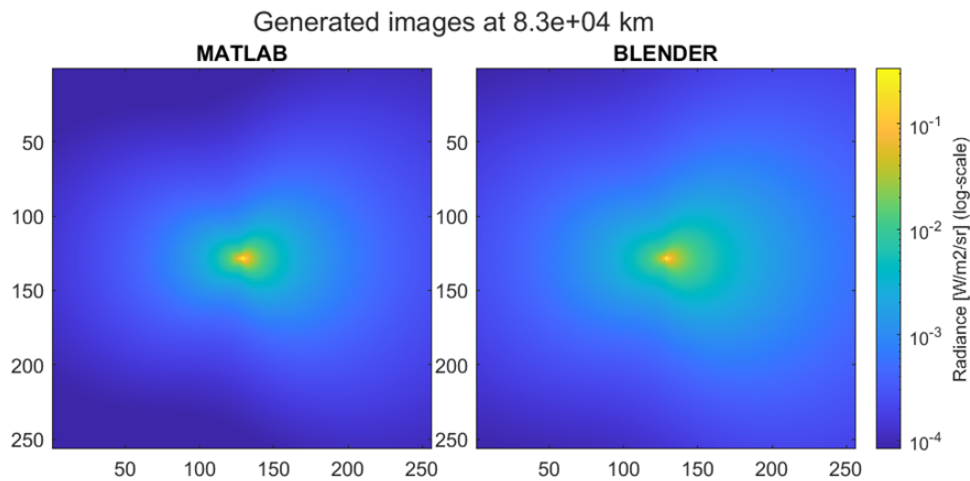


Figure 7: Radiance of the synthetic nucleus and coma from the CPU-based Matlab approach (left) and the GPU-game engine based approach (right) at a distance of  $8.3 \times 10^4 km$ . Both are false color, logarithmic scale

With the UBPGE/Blender approach it is possible to add several features to the dust model, notably emissive dust jets and complex nucleus terrain. An example of such additions is shown in Figure 8 (here the distance to the nucleus is closer than the planned Comet-I closest approach for visualization purposes).



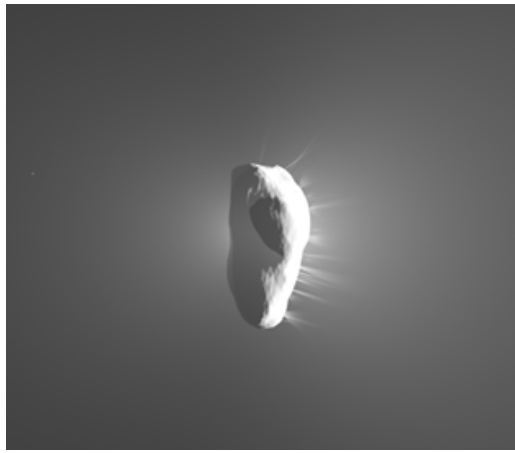


Figure 8: Example of the nucleus of comet Halley rendered with UPBGE at a distance of 200km showing an example of directional jets.

Several additions could be added to the model in the future, such as:

- Cometary tail and bow shock at far range
- Individual particles at close range
- Shadow casting of the nucleus onto the coma.

It should be noted that these additions could potentially hinder the near real time capability of the implementation, and thus should be an on-demand addition that can be toggled on and off.

## 5 UPBGE AND OLED SCREEN COMBINATION

The flexibility of the developed software in combination with the DOGSE allows us to expose the navigation camera to a wide variety of test scenarios for the Comet-I mission. The pictures in Figure 9 show the rendered comet at various distances, as imaged by the navigation camera (in automatic shutter mode) inside the DOGSE. Stars are only visible at far distance, where the comet is dim enough to be of a comparable magnitude.

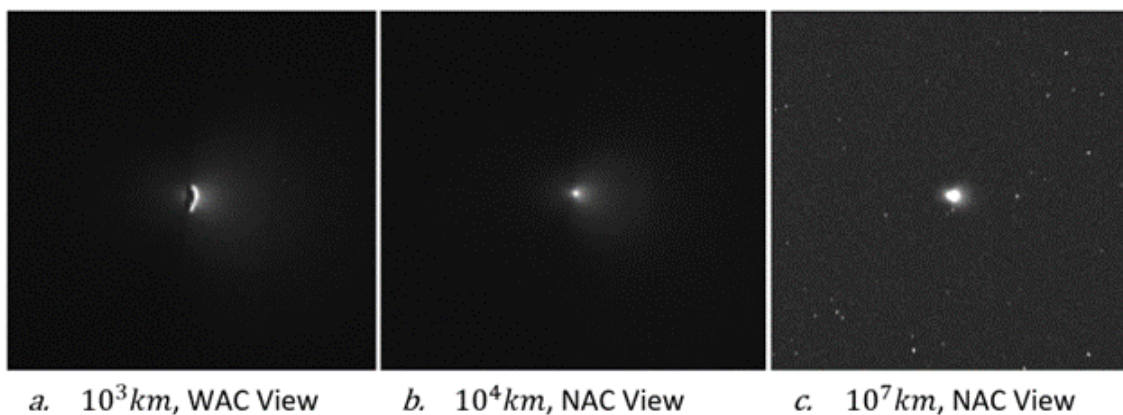


Figure 9: Synthetic images of a comet at different distances. Exposure and gain have been adjusted for visualization. The images are generated using the nucleus of Halley's comet and the standard EDCM coma model.

Figure 10 shows a synthetic image of a comet nucleus (based on 67P/Churyumov-Gerasimenko) with jets imaged in the DOGSE. While not directly useful for the navigation camera analysis, it indicates what the comet may look like in the field of view of the main image sensor (the comet camera “CoCa” instrument). Comparison of the synthetic images with the mission photos from the Giotto and Rosetta missions (Figure 3 and Figure 2) show great resemblance both at far and short range.



Figure 10: Synthetic image of the nucleus of 67P/Churyumov-Gerasimenko with directional jets imaged with a tight CoCa-like field of view around closest approach

## 5.1 Simulation goals

The main use case of the game engine-based model is to enable fast replay of trajectory scenarios. Later, it will be used in full closed HIL simulation. The goals of the simulations are:

- To understand the effect of various imaging parameters.
- To assess the performance of the centroiding of the comet in terms of angular error and noise.
- To test the behaviour of the camera in varying environmental conditions, such as varying nucleus size and dust activity.

## 5.2 Single simulation result

Figure 11 shows an example of a single simulation run with the captured region of interest (ROI) around the comet stitched on a single frame. The ROI is a sub-sample of the larger image downloaded to reduce latency compared to full frame access. Only one measurement each 4 seconds is shown here. The red circle mark the measured centroid and the size represents the integrated flux.

Figure 12 shows the angular errors (alpha shift and beta shift) in degrees between the measured centroid from the camera in the DOGSE and the true nucleus centre. In addition the figure shows the angular error between the position of the brightest pixel on the rendered scene and the true nucleus centre. A conversion (not detailed here) between pixel coordinates and angular, camera space coordinates has been executed on each measurement.

The angular error is shown to be less than the nucleus radius which means that the line of sight vector from the camera falls on the nucleus surface. With this relatively low error, the CoCa instrument will be able to successfully image the nucleus surface during the whole approach assuming correct filtering and navigation sequences. It should be noted that these results are preliminary and are yet neither fully representative of the true camera behavior or of the comet radiation model.

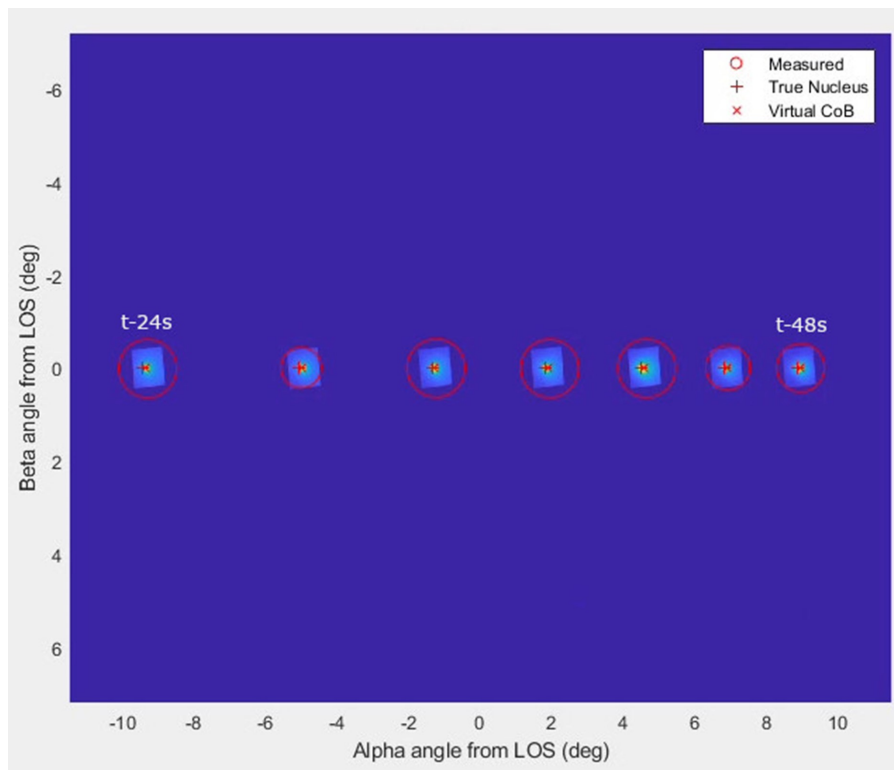


Figure 11: A simulation run with the captured region of interest (ROI) around the comet stitched on a single frame. Red circles show the measured centroid and their size represent intensity. The stitching is composed of images captured every 4 seconds.

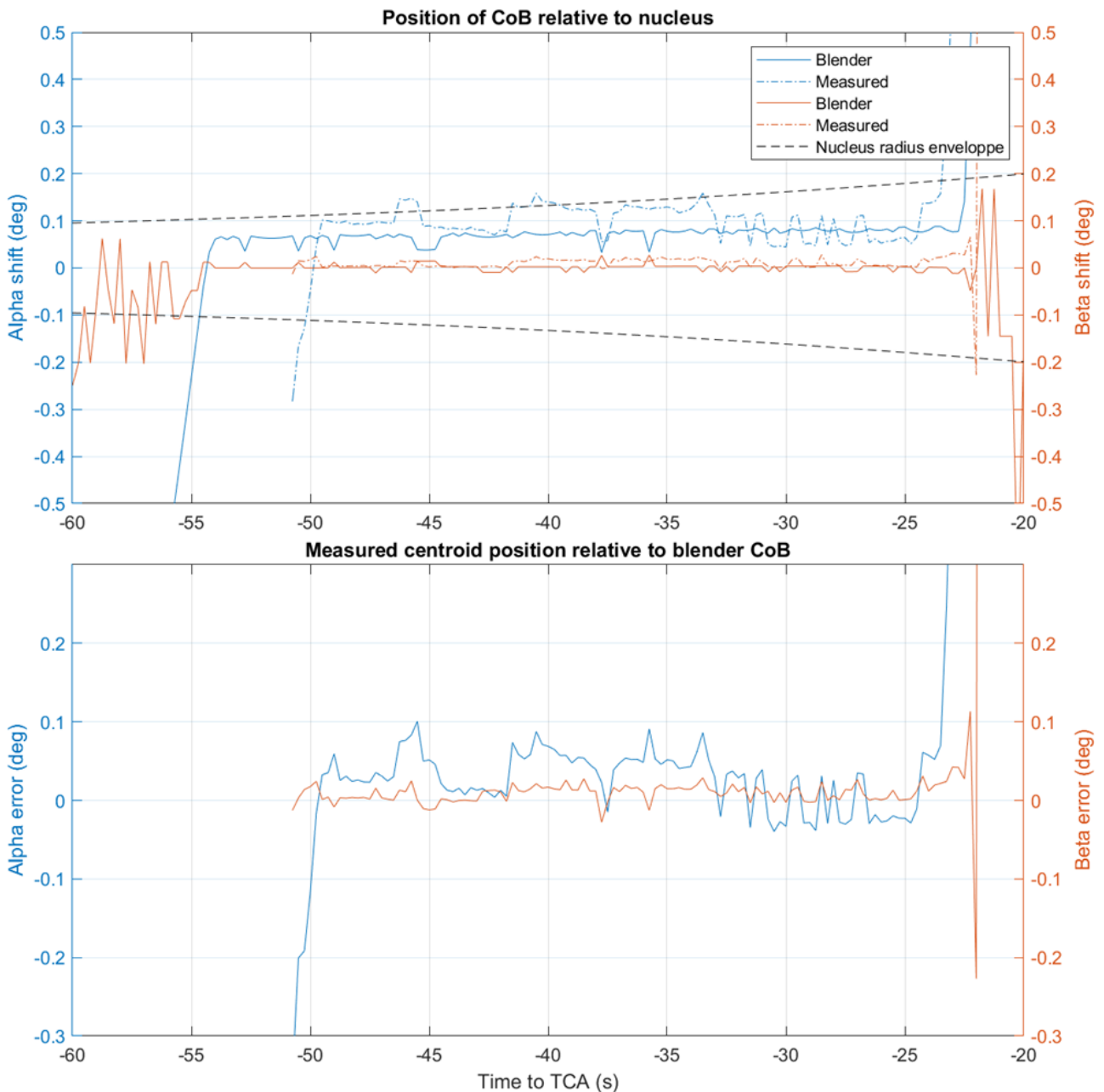


Figure 12: Upper plot: Angular errors between measured center of brightness (CoB) and true nucleus center. Dashed lines are the errors between the CoB reported by the DPU and the true nucleus center. Solid lines are the errors between the brightest pixel in the scene and the true nucleus center. Lower plot: angular errors between the DPU measured CoB and the brightest pixel in the rendered scene.

### 5.3 Varying coma activity

With this tool it is possible to investigate the response of the camera to different dust environments. The cometary activity can be artificially increased or decreased by multiplying the standard EDCM coma dust density by a given percentage. Figure 13 shows the angular errors, the response of the shutter and the power spectral density for a simulation run using a 0%, 50%, 100% (standard EDCM) and 150% coma dust activity model and varying jet activity. The values are still preliminary but the general trend shows that comets with higher dust activity tend to degrade the performance of the navigation camera at close range, both in term of mean angular error and angular noise. Very bright jets

("coma-D150J10" green case) can further degrade the precision.

This trend may not be the same at far range, where a bright coma could help the determination of the centroid by increasing the signal-to-noise ratio. Further studies are needed with a focus on the ability of the camera to discriminate the comet from the background stars.

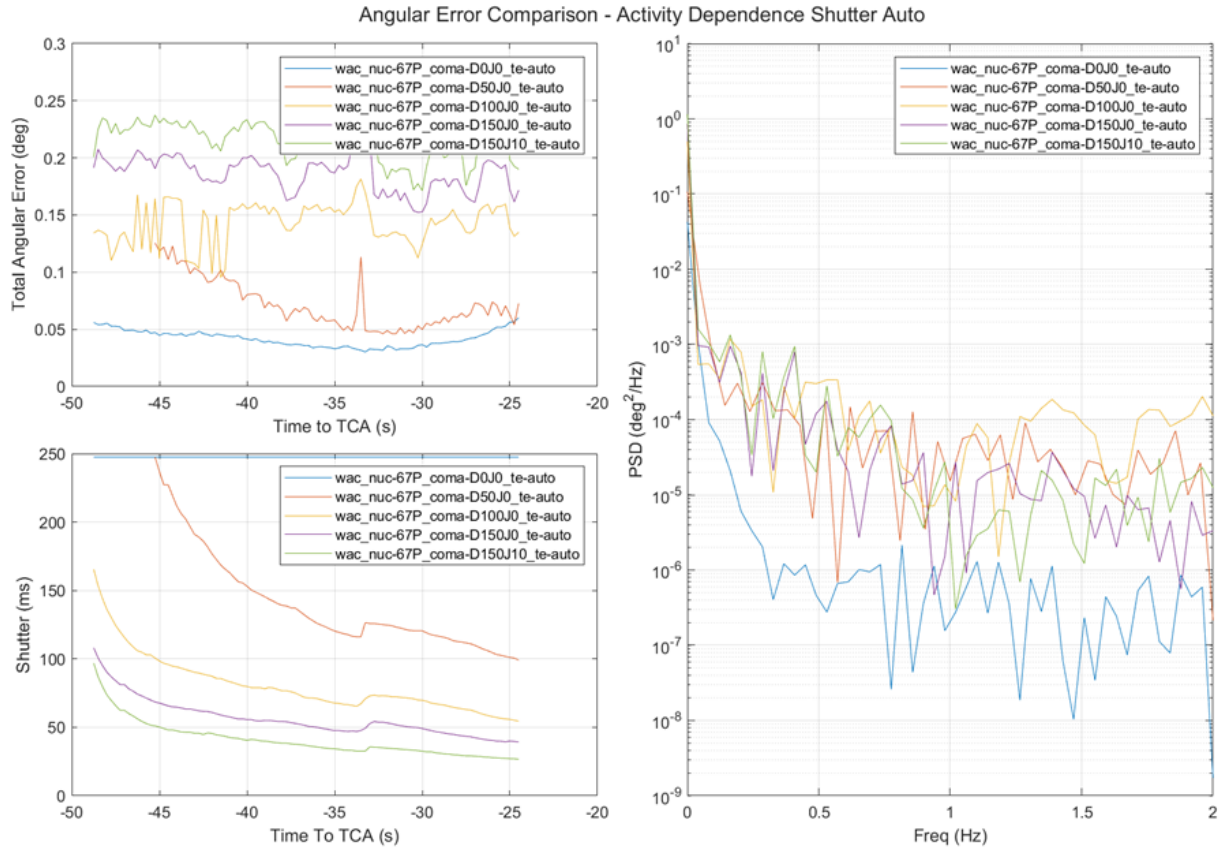


Figure 13: Cometary activity sweep study. Shows angular errors, the response of the shutter and the power spectral density for a simulation run using a 0%, 50%, 100% (standard EDCM) and 150% coma dust activity model. "DXX" denotes the coma percentage relative to the median strength (100%), "JXX" denotes the jet strength parameter. The standard EDCM coma is "coma-D100J0", all others are variations of this model and only coma-D150J10 includes jets.

## 6 CONCLUSION

This paper has introduced the versatile Dynamic Optical Ground Support Equipment (DOGSE) system for high fidelity virtual scene generation and the currently ongoing work to updated the functionality to simulate test scenarios for the Comet-I mission.

Using the Engineering Dust Coma Model (EDCM) we have developed two methods for generating synthetic images of an arbitrary comet nucleus and coma at any distance against an accurate projection of the starry sky. Comparison between methods and with photos obtained by the Giotto and Rosetta missions have shown good representativeness of the synthetic images.

We have shown that the DOGSE system can accurately display the synthetic scenes to the image sensor and that adding a game-engine based rendering approach enable near real time simulation ca-

pabilities and flexibility in the model. This allows for a rapid turn-around when the need for a new test-case arises of high value for the highly dynamic and complex comet-I mission to an unknown comet.

Preliminary simulations have aided our understanding of the effect of various imaging parameters and allowed us to assess the performance of the centroiding of the comet in terms of angular error and noise. Furthermore, due to the flexibility of the tool and the scalability of the dust activity model, we can test the behaviour of the cameras in different environmental conditions, such as varying the nucleus size, increasing/decreasing the dust activity and adding directional jets.

## REFERENCES

- [1] R. Reinhard, “The giotto mission to comet halley,” *Journal of Physics E: Scientific Instruments*, vol. 20, no. 6, p. 700, Jun. 1987. DOI: 10.1088/0022-3735/20/6/029.
- [2] W. Curdt and H. Keller, “Large dust particles along the giotto trajectory,” *Icarus*, vol. 86, no. 1, pp. 305–313, 1990, ISSN: 0019-1035. DOI: [https://doi.org/10.1016/0019-1035\(90\)90220-4](https://doi.org/10.1016/0019-1035(90)90220-4).
- [3] D. G. Schleicher, R. L. Millis, and P. V. Birch, “Narrowband photometry of comet p/halley: Variation with heliocentric distance, season, and solar phase angle,” *Icarus*, vol. 132, no. 2, pp. 397–417, 1998, ISSN: 0019-1035. DOI: <https://doi.org/10.1006/icar.1997.5902>. [Online]. Available: <https://www.sciencedirect.com/science/article/pii/S0019103597959029>.
- [4] M. Rayman, P. Varghese, D. Lehman, and L. Livesay, “Results from the deep space 1 technology validation mission,” *Acta Astronautica*, vol. 47, no. 2, pp. 475–487, 2000. DOI: 10.1016/S0094-5765(00)00087-4.
- [5] ESA, *Giotto Data: GIO-C-HMC-3-RDR-HALLEY, VI.0*, [Online; accessed 2022-10-24], 2004. [Online]. Available: <https://archives.esac.esa.int/doi/html/data/planetary/GIOTTO/GIO-C-HMC-3-RDR-HALLEY.html>.
- [6] W. Blume, “Deep impact mission design,” *Space Science Reviews*, vol. 117, no. 1, pp. 23–42, Mar. 2005. DOI: 10.1007/s11214-005-3386-4.
- [7] E. S. Agency, “Rosetta-NAVCAM,” Tech. Rep., Aug. 2013, Planetary Science Archive Interface Control Document. [Online]. Available: <https://archives.esac.esa.int/psa/ftp/INTERNATIONAL-ROSETTA-MISSION/NAVCAM/RO-E-CAL-NAVCAM-2-EAR2-V1.0/DOCUMENT/RO-SGS-IF-0001.PDF>.
- [8] D. Brownlee, “The stardust mission: Analyzing samples from the edge of the solar system,” *Annual Review of Earth and Planetary Sciences*, vol. 42, no. 1, pp. 179–205, 2014. DOI: 10.1146/annurev-earth-050212-124203.
- [9] B. R. Kent, *3D Scientific Visualization with Blender® (2053-2571)*. Morgan & Claypool Publishers, 2015, ISBN: 978-1-6270-5612-0. DOI: 10.1088/978-1-6270-5612-0. [Online]. Available: <https://dx.doi.org/10.1088/978-1-6270-5612-0>.
- [10] C. Opitom, E. Jehin, J. Manfroid, D. Hutsemékers, M. Gillon, and P. Magain, “Trappist photometry and imaging monitoring of comet c/2013 r1(lovejoy): Implications for the origin of daughter species,” *Astronomy & Astrophysics*, vol. 584, Jul. 2015. DOI: 10.1051/0004-6361/201526427.

- [11] L. V. Ksanfomality, “Comparison of some characteristics of comets 1p/halley and 67p/churyumov–gerasimov from the vega and rosetta mission data,” *Solar System Research*, vol. 51, pp. 225–242, Jul. 2017. DOI: 10.1134/S0038094617030054.
- [12] M. Taylor, N. Altobelli, B. J. Buratti, and M. Choukroun, “The rosetta mission orbiter science overview: The comet phase,” *Philosophical Transactions of the Royal Society A: Mathematical, Physical and Engineering Sciences*, vol. 375, no. 2097, p. 20160262, 2017. DOI: 10.1098/rsta.2016.0262.
- [13] Blender Foundation, *Blender - a 3D modelling and rendering package*, 2018. [Online]. Available: <http://www.blender.org>.
- [14] ESA, “Comet Interceptor Assessment of Mission to Intercept a Long Period Comet or Interplanetary Object,” ESA/ESTEC, Tech. Rep., Dec. 2019. [Online]. Available: <https://sci.esa.int/web/future-missions-department/-/cdf-study-report-comet-interceptor>.
- [15] ESA, “Comet interceptor red book,” ESA, Tech. Rep., Apr. 2022. [Online]. Available: <https://www.cosmos.esa.int/documents/3760686/3760706/Comet+Interceptor+Red+Book.pdf/dfa9634f-b15b-e918-17b5-5a8523149ea7?t=1664524062069>.
- [16] R. Marschall, V. Zakharov, C. Tubiana, *et al.*, *Engineering dust coma model (edcm) for esa’s comet interceptor mission to a dynamically new comet (4.2.0)*, 2022. DOI: 10.5281/zenodo.6906815.
- [17] Marschall, R., Zakharov, Vladimir, Tubiana, Cecilia, *et al.*, “Determining the dust environment of an unknown comet for a spacecraft flyby: The case of esa’s comet interceptor mission,” *A&A*, vol. 666, A151, 2022. DOI: 10.1051/0004-6361/202243648.